

# Numerical analysis of natural convection around a vertical channel in a rectangular enclosure

J. P. Liu, W. Q. Tao

313

**Abstract** Numerical computations were performed for the heat transfer and fluid flow characteristics of an internal vertical channel composed by a pair of parallel plates situated in a rectangular enclosure, with the inner plates and the bounding wall of the enclosure maintained at uniform but different temperatures. Natural convection occurred in the air which occupied the enclosure space. The plates were symmetrically arranged. The dimensionless channel width  $S$  was varied parametrically. The Rayleigh numbers ranged from 102 to 107. Static bifurcation was found in this configuration. The bifurcation is related to the flow pattern transition from single-vortex structure to double-vortex structure or vice versa. Comparison with the empirical correlations obtained for a vertical plate and a channel in an infinite space showed that the heat transfer process of the plates and the channel was deteriorated by the existence of the enclosure.

*Numerische Ermittlung der natürlichen Konvektion um einen vertikalen Kanal in einer rechteckigen Kammer*

**Zusammenfassung** Aus numerischen Berechnungen wurde das Wärmeübergangs- und Strömungsverhalten eines aus zwei parallelen Platten gebildeten Vertikalkanals ermittelt, der sich symmetrisch angeordnet in einer rechteckigen Kammer befindet. Kanal- und Kammerwände haben gleichförmige, jedoch unterschiedliche Temperaturen. In der luftgefüllten Kammer herrscht freie Konvektion. Die dimensionslose Kanalbreite  $S$  wurde als Parameter variiert, wobei die Rayleigh-Zahlen zwischen 102 und 107 lagen. Für die beschriebene Konfiguration wurde statische Bifurkation festgestellt, welche sich im Strömungsbild durch den Übergang von der Einzel- zur Doppelwirbelstruktur und umgekehrt dokumentiert. Der Vergleich mit empirischen Beziehungen für eine vertikale Platte und einen Kanal im unbegrenzten Raum ergab, daß der Wärmeaustausch an Platte und Kanal durch den Kammeranschluß behindert wird.

Received 24 August 1995

J. P. Liu  
W. Q. Tao  
School of Energy and Power Engineering  
Xi'an Jiaotong University  
Xi'an, Shaanxi 710049, PRC

This work was supported by the Natural National Science Foundation of China

Correspondence to: W. Q. Tao

## Nomenclature

$a$	thermal diffusivity
$b$	half width of the enclosure
$B$	dimensionless half width of the enclosure
$F_1$	dimensionless mass flow through half width of the channel
$h$	height of the channel plate
$k_f$	fluid thermal conductivity
$k_s$	solid thermal conductivity
$\tilde{K}$	relative thermal conductivity
$l$	distance from the top of the plate to the top wall of the enclosure, i.e., distance from the bottom of the plate to the bottom wall of the enclosure
$L$	dimensionless of $l$
$M_{res}$	mass residual
$Nu_{CH}$	channel Nusselt number
$Nu_{CH}$	outside channel Nusselt number
$Nu_l$	local Nusselt number
$Nu_1$	average inside surface Nusselt number
$Nu_0$	average outside surface Nusselt number
$p'$	effective pressure
$P$	dimensionless pressure, defined as $P = p' / [(\rho(RaPr)/(a/h)^2)]$
$Pr$	Prandtl number
$Ra$	Rayleigh number based on the height of the plate, $h$
$Ra_{CH}$	channel Rayleigh number
$s$	channel width
$S$	dimensionless channel width, $s/h$
$t$	time
$T$	temperature
$T_h$	temperature of the internal plate
$T_c$	temperature of the enclosure surface
$u, v$	velocity components in $x, y$ -direction
$U, V$	dimensionless velocities, $U = u/u_r, V = v/u_r$
$u_r$	reference velocity, defined as $(RaPr)^{1/2}/(a/h)$
$x, y$	coordinates
$X, Y$	dimensionless coordinates, $X = x/h, Y = y/h$

## Greek symbols

$\alpha_i$	heat transfer coefficient
$\beta$	volume expansion coefficient
$\delta$	thickness of the plates
$\nu$	kinetic viscosity
$\rho$	density of the fluid
$\tau$	dimensionless time, defined as $u_r t/h$
$\phi$	dimensionless temperature, defined as $(T - T_c)/(T_h - T_c)$

## 1 Introduction

Vertical channel formed by two parallel plates or fins is a frequently encountered configuration in thermal engineering equipment, for example, the finned exchanger, the collector of solar energy, the core of nuclear reactors, and the cooling device of electronic and micro-electronic equipment. Elenbass [1] was the first to conduct a detailed study for the thermal characteristics of one such configuration. Since then, extensive investigations have been performed on this subject. Bar-Cohen and Rohsenow [2] studied the heat transfer characteristics of such configuration analytically and experimentally, and obtained relations which could be used either in fully developed circumstance or developing case. Guo and Wu [3] considered the variable properties of fluids and obtained the critical heat flux for one given channel. Other related works may be found in Nakayama et al. [4], Sparrow and Azevedo [5], Chang and Lin [6] and Naylor et al. [7].

Unlike the previous works, the emphasis of the present paper is put on the channel which is located in a rectangular enclosure. In fact, for many circumstances such as the cooling of electronic equipment, this case is more practical than it is in the infinite space. The characteristics of the natural convection will be seriously influenced by the existing of the enclosure, because the fluid can not be cooled perfectly before it enters the inlet of the channel and the flow leaving the channel is restricted. On the other hand, this problem belongs to the category of natural convection in enclosure with internal isolated islands, which has received ever-increasing attention in recent years. Here by the term internal isolated islands we mean the solid bodies which situate in the flow field and are not bounded by any part of the computation domain boundary. A review on this category of natural convection in enclosure has been made by Wang et al. [8] recently and will not be restated in this paper. Here only the results obtained by Adlam [9] and Shyy and Rao [10] will be briefly introduced. Adlam [9] performed computations of two-dimensional transient natural convection in cavities where there were one or several internal isolated bodies. Among the configurations studied was the cavity with two internal vertical thick plates, which were set in the enclosure symmetrically and heated to a constant temperature with the surrounding walls of the cavity cooled to a constant temperature. Only one case (Rayleigh number based on the cavity height was 106 and Prandtl number was 5.39) was computed. It was found that the flow in the cavity was symmetrical about the vertical midplane of the cavity, and the stream function did not approach a constant value as time increased. It was thus concluded that there was no time-independent solution of flow for the cavity studied. Recently, Shyy and Rao [10] performed a transient numerical simulation for a similar configuration with zero plate thickness for which the Grashof number based on the channel half width was 105 and Prandtl number was 0.71, but the cavity had adiabatic top and bottom walls with its two vertical surfaces maintained at constant temperatures. Their results showed that when time approached infinite, steady state solution did exist. In the present work, investigation has been carried out on the steady-state situation, with Rayleigh number and the distance between the two vertical plates (i.e., channel width) as the two parameters. The major purposes of this study are: (1) to

compare the heat transfer characteristics between the natural convection around an enclosure channel and that in an infinite space; (2) to investigate parametrically the effect of the channel width on the heat transfer characteristics; (3) to examine whether there is a bifurcation in the steady-state solutions in a wide range of the Rayleigh number and the channel width

## 2 Mathematical formulation and numerical method

A schematic diagram of the problem studied is shown in Fig. 1. As seen there, a channel with height  $h$  and width  $2s$  is situated symmetrically in the enclosure, therefore only half of the enclosure is taken as the computational domain. The entire boundary of the rectangular enclosure is at uniform and constant temperature ( $T_c$ ), while the channel walls are of a higher and uniform temperature  $T_h$ . The configuration studied may be defined by four geometric parameters:  $s/h$ ,  $l/h$ ,  $\delta/h$  and  $b/h$ . Besides, the Rayleigh number and the Prandtl number have to be added, yielding total of six parameters that must be specialized for each case studied. With the cooling technique of microelectronic equipment as its application background, the six parameters are chosen as follows. The Prandtl number is fixed (0.7),  $1/h$  and  $b/h$  are taken as 0.75 and 1. The value of  $\delta/h$  is 0.03. The variation range of the Rayleigh number based on the channel height is from 102 to 107, and that of  $s/h$  form 0.1 to 0.3. Since one purpose of the present study is to investigate the effect of the channel width  $S$  while other conditions remain the same, the channel height rather than the channel width is taken as the characteristic length for making the dimensionless geometric parameters and for the Rayleigh number. When comparison is made with the results for infinite space where the channel width is adopted as the characteristic length, the channel height based Rayleigh number will be converted to channel width based one.

The following assumptions are adopted in the numerical analysis:

1. The fluid in the enclosure is of Boussinesq type.
2. The fluid flow and heat transfer is two-dimensional, laminar and in steady-state.
3. The dissipation term in the energy equation is neglected.

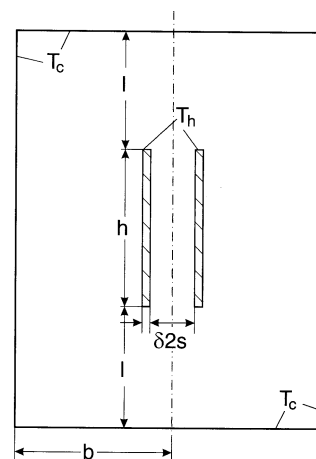


Fig. 1. Schematic diagram of configuration studied

Using the definitions given in the nomenclature, we may obtain the following dimensionless governing equations:

$$\frac{\partial U}{\partial \tau} + U \frac{\partial U}{\partial X} + V \frac{\partial U}{\partial Y} = -\frac{\partial P}{\partial X} + \frac{Pr}{\sqrt{Ra Pr}} \left( \frac{\partial^2 U}{\partial X^2} + \frac{\partial^2 U}{\partial Y^2} \right) \quad (1)$$

$$\frac{\partial V}{\partial \tau} + U \frac{\partial V}{\partial X} + V \frac{\partial V}{\partial Y} = -\frac{\partial P}{\partial Y} + \frac{Pr}{\sqrt{Ra Pr}} \left( \frac{\partial^2 V}{\partial X^2} + \frac{\partial^2 V}{\partial Y^2} \right) + \phi \quad (2)$$

$$\frac{\partial \phi}{\partial \tau} + U \frac{\partial \phi}{\partial X} + V \frac{\partial \phi}{\partial Y} = -\frac{K}{\sqrt{Ra Pr}} \left( \frac{\partial^2 \phi}{\partial X^2} + \frac{\partial^2 \phi}{\partial Y^2} \right) \quad (3)$$

$$\frac{\partial U}{\partial X} + \frac{\partial V}{\partial Y} = 0 \quad (4)$$

The boundary conditions are as follows

at the wall of the enclosure:

$$U = V = \phi = 0 \quad (5)$$

at the symmetrical line:

$$U = \frac{\partial V}{\partial X} = \frac{\partial \phi}{\partial X} = 0 \quad (6)$$

In addition, the following conditions must be satisfied for the internal solid plate:

$$U = V = 0, \quad \phi = 1 \quad (7)$$

The governing equations were then discretized by the finite volume approach. The power-law scheme was adopted for the discretization of the convection–diffusion terms. The SIMPLE algorithm was used. Special attention was paid to the treatment of the isolated solid region. In our work, the coefficients of the discretization equations were properly assigned to confirm the additional condition (7) in the solid region. Besides, the relative thermal conductivity  $K(k_s/k_f)$  takes the value of 1 in the fluid region and a very large value in the solid region. For details, the literature of Yang and Tao [11] may be referred.

Heat transfer from the vertical plate may be correlated by the local Nusselt number based on the difference between the heated wall temperature and cooled wall temperature as follows:

$$Nu_1 = \frac{\alpha_1 h}{k_f} \quad (8)$$

where the local heat transfer coefficient is defined as

$$\alpha_1 = -\frac{k_f}{T_h - T_c} \left( \frac{\partial T}{\partial n} \right)_W \quad (9)$$

The average Nusselt numbers of the channel plate are determined by integration over the surface of the vertical plate, and can be expressed as

$$Nu_1 = \frac{1}{h} \sum_{\text{INNER}} Nu_1 \Delta h_1 \quad (10)$$

$$Nu_0 = \frac{1}{h} \sum_{\text{OUTER}} Nu_1 \Delta h_1 \quad (11)$$

where  $\Delta h_1$  is the surface element on the vertical plate and  $h$  is its total surface area, i.e., the height of the channel. In Eq. (10),

**Table 1.** Mesh independency check ( $S=0.1$ )

Grid number	$Ra: 104$		$Ra: 106$	
	$Nu_1$	$Nu_0$	$Nu_1$	$Nu_0$
24 × 24	1.452	4.473		
36 × 36	1.410	4.210	10.06	10.34
48 × 48	1.418	4.170	9.76	9.97

the subscript “I” means that the summation is carried out for the element on the channel inside surface, while the subscript “O” presents the summation for the channel outside surface.

The dimensionless half mass flow in the channel is defined as

$$F_1 = \int_0^S \rho V dx = \sum V_i \Delta X_i \quad (12)$$

where  $\Delta X_i$  is the surface element on the channel cross-section.

The Rayleigh number is determined by the following equation:

$$Ra = \frac{g\beta(T_h - T_c)h^3}{\nu\alpha} \quad (13)$$

The iteration procedure was ceased when both of the following conditions were satisfied:

$$\frac{M_{\text{res}}}{G} \leq 2 \times 10^{-5} \quad (14)$$

$$\left| \frac{Nu_1^{(k+1)} - Nu_1^{(k)}}{Nu_1^{(k+1)}} \right| \leq 1 \times 10^{-5} \quad (15)$$

where

$$G = \int_0^B |V| dY \quad (16)$$

The value  $M_{\text{res}}$  is the mass residual of the whole solution domain,  $Nu_1^{(k)}$  and  $Nu_1^{(k+1)}$  are the average Nusselt numbers of the two successive iterations.

The code developed by the present authors was first used to predict the average Nusselt number of the confined channel investigated by Shyy and Rao [10] with a grid system of 40 × 40, and a value of 4.6388 was achieved, which was in good agreement with the result provided by Shyy and Rao [10].

The grid layout was characterized by an equal distribution of grid points in the  $Y$  direction and a non-equal distribution in the  $X$  direction, which had the grid points concentrated near the solid plate, but sparse far from the plate. Networks of different grid number were used in the preliminary computation to find out an appropriate grid system (Table 1). The compromise between numerical accuracy and computer sources led to the use of the 36 × 36 grid system.

### 3 Results and discussion

#### 3.1 Transient vs. steady-state simulation

Before the steady-state numerical simulations, the unsteady process of the flow development from zero initial field was

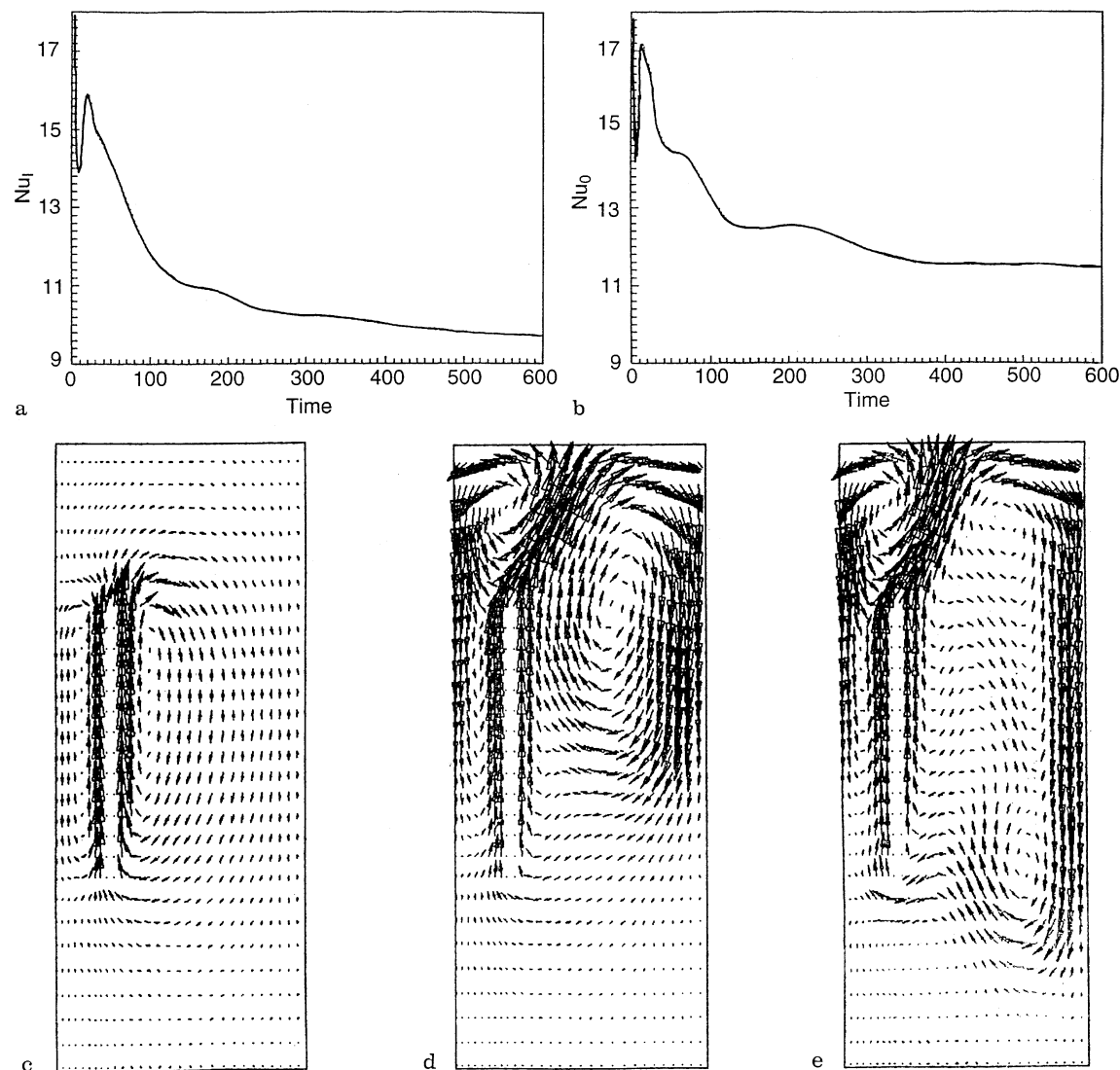


Fig. 2a-e. Prediction of unsteady process from zero initial field (for  $S=0.2$ ,  $Ra=106$ ). a the history of  $Nu_i$  to time; b the history of  $Nu_o$  to time; c velocity field at time=5; d velocity field at time=30; e velocity field at time=500

simulated. Such investigation with insulated top and bottom wall was performed by Shyy and Rao [10]. Our case different from that of Shyy and Rao by the isothermal and cold top and bottom wall. The work performed by Adlam [9] showed that the steady flow in such kind of configuration did not exist. The case we studied had dimensionless half channel width of 0.2 and  $Ra$  of 106. The mesh used was  $89 \times 86$ , which was the maximum grid numbers our personal computer could offer. The time step was 0.01 at beginning and gradually increase when the flow was developing. Finally, a time step of 0.25 was used when the flow was approaching steady. The results are shown in Fig. 2. Figures 2a and b show the history of the average Nusselt number of the inside and the outside channel wall, illustrating the existence of the steady flow. Figures 2c-e show the developing process of velocity field. The numerical values of  $Nu_i$  and  $Nu_o$  when time approaching infinite agree with our steady-state solutions quite well. In the following presentation, the results were all achieved by steady-state computation.

### 3.2 Flow patterns and isotherms

The flow patterns and isotherms are drawn for three typical Rayleigh numbers,  $Ra=5 \times 10^2$ ,  $1 \times 10^5$  and  $2 \times 10^6$  for  $S=0.1$ . These are presented in Figs. 3-5. As it can be observed in Fig. 3, for the low Rayleigh number cases (as  $Ra=500$ ), the velocity field indicates that the conduction mode is predominated. For this case, the flow field consists of single vortex in the half domain, part of which is situated between the channel outside surface and enclosure vertical wall, and the other covers the channel plate. A stagnation point is located at the center part of the vortex, a bit higher than the mid-height position of the cavity. When the Rayleigh number increases to as high as 105, the natural convection has become predominated, as witnessed by the temperature inversion shown in Fig. 4b. At this level of Rayleigh number, around the vertical plate, a boundary-layer flow has been formed, as this can be observed from the isotherm distribution around the plate (Fig. 4b). The over-all flow pattern in the enclosure is also of

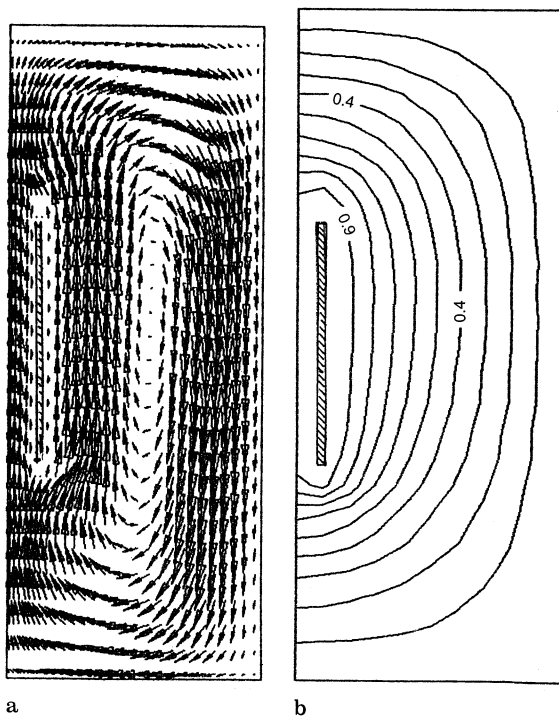


Fig. 3a, b. Predicted velocity field and isotherms ( $Ra=5 \times 10^2$ ).  
a velocity field; b isotherms

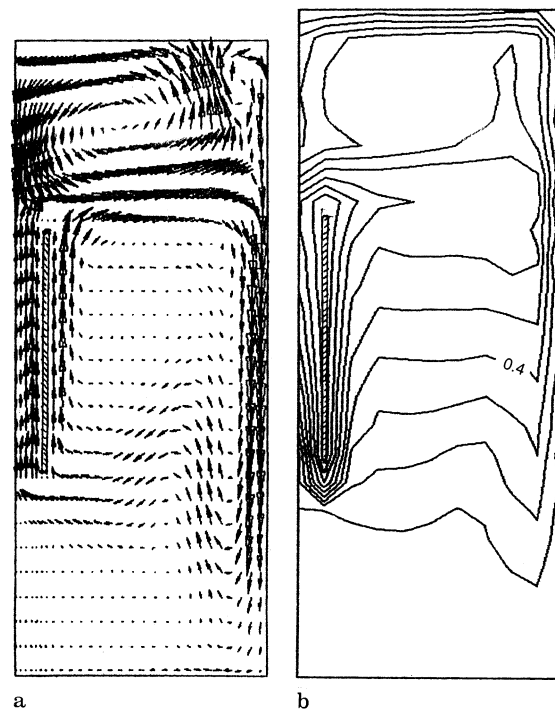


Fig. 5a, b. Predicted velocity field and isotherms ( $Ra=2 \times 10^6$ ).  
a velocity functions; b isotherms

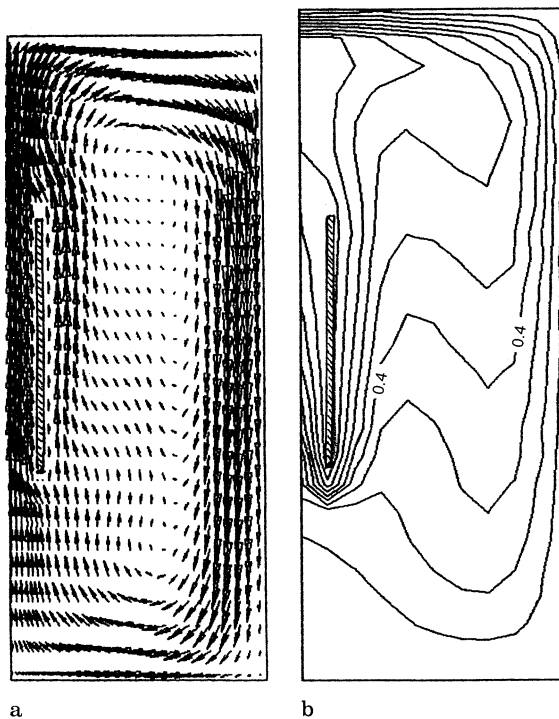


Fig. 4a, b. Predicted velocity field and isotherms ( $Ra=1 \times 10^5$ ).  
a velocity field; b isotherms

single-vortex type (Fig. 4a). But the stagnation point moves up. A further increase in the Rayleigh number leads to a separation of the entire vortex, and thus a double-vortex structure is formed. The flow field now consists of two vortices, one at the top position and the other underneath (Fig. 5a). For this case,

apart from a narrow region around the vertical plate, where boundary-layer type velocity field may be observed, the major part of the space between the plate and the vertical wall has parallel vertical velocity and zero horizontal velocity, indicating the strong effect of the natural convection.

It is found that the mechanism of the transition from the single-vortex pattern to the double-vortex structure is very complicated. For  $s=0.1$ , our preliminary investigations show that the static bifurcation in flow pattern does exist. The method of increasing or decreasing the Rayleigh number gradually is used to reveal the Rayleigh number range within which the static bifurcation exists. In such method, the velocity and temperature fields calculated for a lower or higher Rayleigh number was used as the initial fields for the computation of the next Rayleigh number. It is found that when the Rayleigh number is increasing from a lower value for which the flow is of single-vortex type, the single-vortex structure can exist up to  $Ra=8.5 \times 10^5$  for  $S=0.1$ , while when the Rayleigh number is decreasing from a higher value for which the double-vortex structure has already existed, this structure may remain to a Rayleigh number as low as  $6.5 \times 10^5$ . When the Rayleigh number is between  $6.5 \times 10^5$  and  $8.5 \times 10^5$ , either of these two flow structures may appear. The average Nusselt number inside the channel differs about 20% between the two different solutions. The diagram of bifurcation for the average Nusselt number of the channel inside surface is shown in Fig. 6. As an example, the flow patterns and isotherms of the two structures for  $Ra=7.5 \times 10^5$  are presented in Fig. 7. Obviously, the existence of the top vortex in the double-vortex structure prevents the outflow from the channel, hence, the heat transfer of the channel is deteriorated.

In the following presentation, in order that the results are in the safe side, the solution of the double-vortex structure will

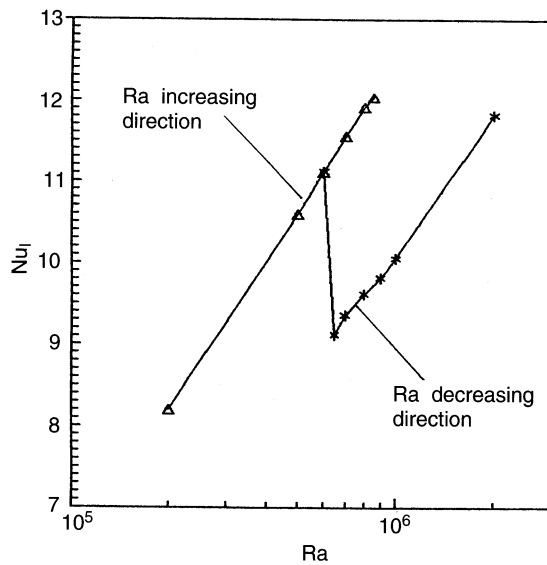


Fig. 6. Bifurcation diagram for  $S=0.1$

be used when the Rayleigh number is within the range where bifurcation may occur.

### 3.3

#### The heat transfer characteristics

##### 3.3.1 Local heat transfer characteristics

The local Nusselt numbers of the channel inside surface are shown in Fig. 8 for  $Ra=5 \times 10^2$ ,  $1 \times 10^5$  and  $2 \times 10^6$  for  $S=0.1$ . In this figure, the abscissa represents the relative position, defined as  $(y-y_{in})/h$ , where  $y_{in}$  is the ordinate of the channel inlet. According to this diagram, for the case of  $Ra=5 \times 10^2$ , the local Nusselt numbers are very small and almost symmetrically about the mid-height position of the plate distributed along the plate height. When  $Ra$  increases to an order of  $10^5$  or more, the local Nusselt number at the beginning of the channel entrance has its highest value, and then decreases gradually along the height direction of the plate. It can be seen that there is some rise in the local Nusselt number at the exist of the channel at high Rayleigh number. This is caused by the rushing-out effect of the upward stream. This variation trend of the local Nusselt number along the height is consistent with the well-known characteristics of the entrance effect of heat transfer and fluid flow in duct.

##### 3.3.2

#### Comparison with a single vertical plate

The average Nusselt numbers of the channel inside and outside surfaces are shown in Figs. 9 and 10, respectively, with the Rayleigh number as a parameter. In these two figures, the results of the Nusselt numbers of a single plate situated in an infinite space predicted from Churchill's equation [12] are also shown. By carefully inspecting these two figures, the following features may be noted. First, when the Rayleigh number is in the order at  $10^2 \sim 10^3$ , the channel inside average Nusselt numbers are almost constant, independent on the Rayleigh number, indicating the conduction regime of heat transfer. However, when Rayleigh number is beyond this regime, the

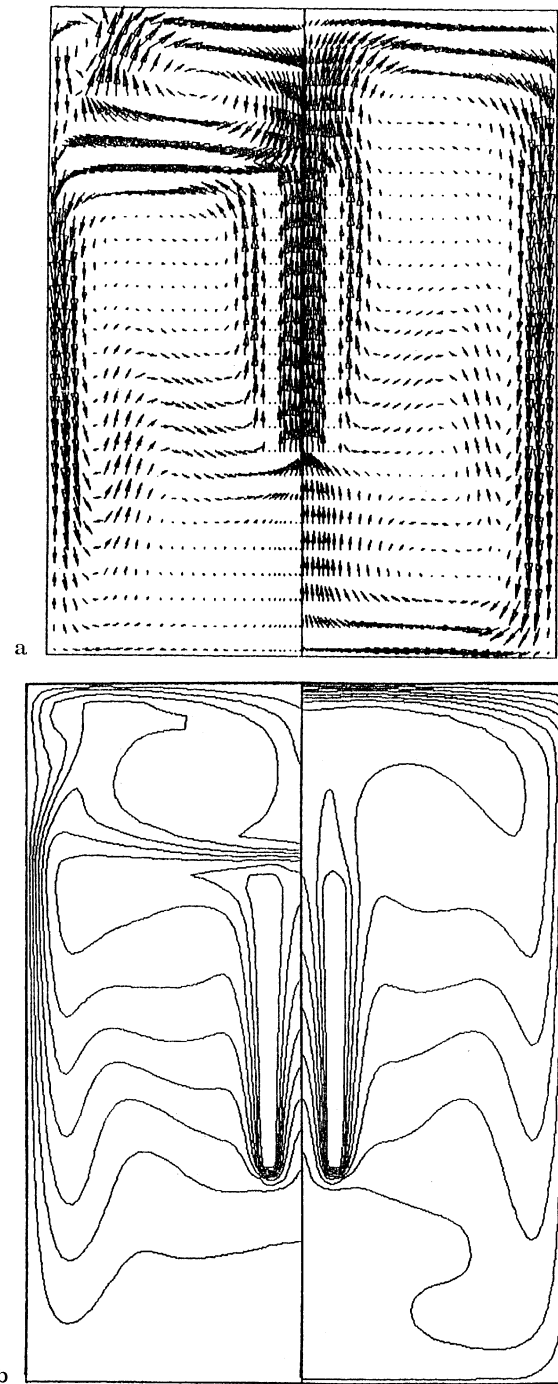


Fig. 7a, b. Velocity field and isotherms for  $(Ra=7.5 \times 10^5)$ . a velocity field (left for double vortex and right for single vortex); b isotherms (left for double-vortex and right for single-vortex)

channel inside Nusselt number increases rapidly with the Rayleigh number. This rapid-increase character is mainly caused by the channel effect. Second, for the channel inside Nusselt number, there is a certain point at the Rayleigh number axis, beyond which its value seems to remain approximately constant in a small range of  $Ra$ , and then with the further increase in  $Ra$ , the average Nusselt number increases gradually. This point is an indication of static bifurcation happening. The corresponding Rayleigh number is the critical Rayleigh

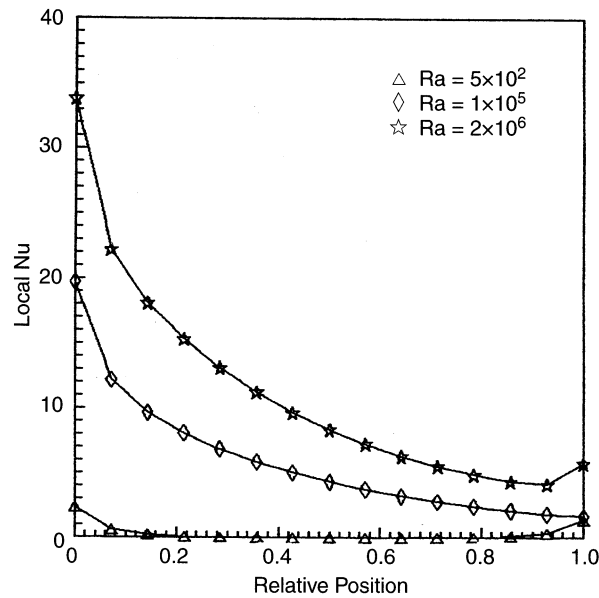


Fig. 8. Local Nusselt number distributions at channel inside surface

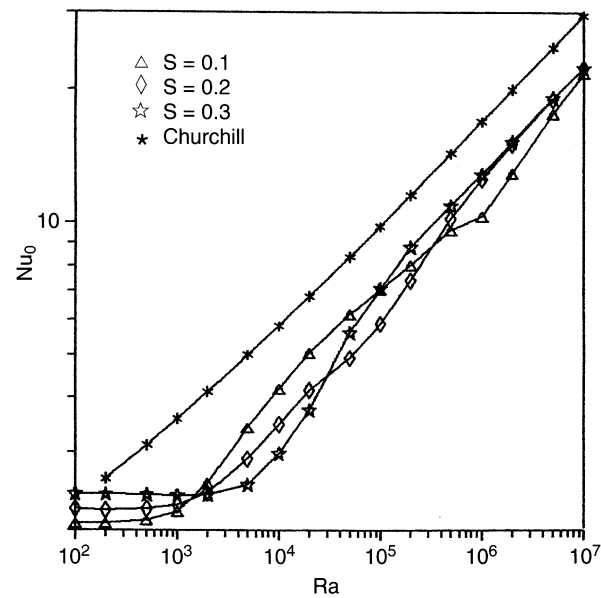


Fig. 10. Channel outside Nusselt number vs. Rayleigh number

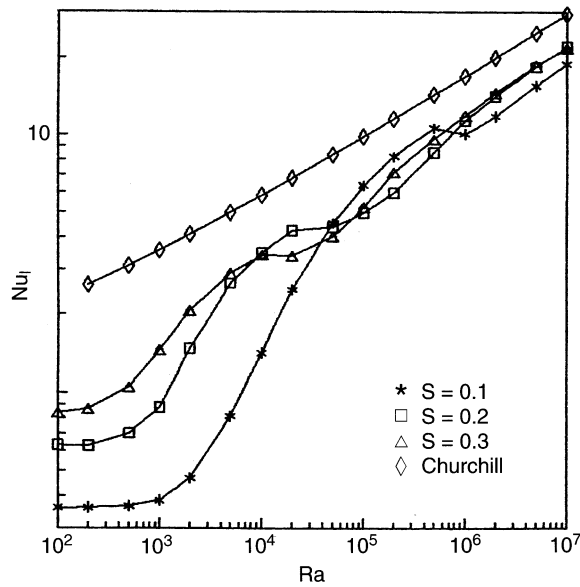


Fig. 9. Channel inside Nusselt number vs. Rayleigh number

number beyond which the static bifurcation may occur. Third, the effect of channel width on the channel inside average Nusselt number is significant in the low Rayleigh number region, a decrease in  $S$  from 0.3 to 0.1 may lead to a decrease in inside Nusselt number of 2 ~ 4 times. However, when the Rayleigh number is beyond  $4 \times 10^4$ , the difference between the inside average Nusselt numbers reduces to about  $\pm 10\%$ . This insensitivity of the channel inside average Nusselt number with the channel height-based Rayleigh number may be interpreted by the fact that for a long vertical channel, the natural convection inside it may become fully developed, and thus the effect of the channel width on the average Nusselt number will disappear. Fourth, the variation trend of the average Nusselt number of the outside surface is qualitatively the same as that of the channel inside Nusselt number. However, the channel

width has much less effect on the average Nusselt number and the bifurcation seems to have little effect. Finally, the heat transfer coefficients of the inside and outside surface of the channel are both lower than that predicted by Churchill's equation for a vertical plate in an infinite space. And with the increase in Rayleigh number, the difference decreases. This observation is qualitatively consistent with the experimental results obtained by Yang and Tao [13], where measurements have been performed for an internal vertical plate in an enclosure, and it has been found that the plate average Nusselt number is lower than that predicted by the Churchill's equation.

### 3.3.3

#### Comparison with the channel in infinite space

In order to make the comparison meaningful, the channel Rayleigh number and the channel average Nusselt number,  $Nu_{CH}$ , are defined:

$$Ra_{CH} = Ra \left( \frac{2s}{h} \right)^4 = 16 Ra S^4 \quad (17)$$

$$Nu_{CH} = 2Nu_i \left( \frac{2s}{h} \right) = 4Nu_i S \quad (18)$$

For the vertical channel in an infinite space, Bar-Cohen and Rohsenow [2] proposed the following correlation:

$$Nu_{CH} = 1 / (576 Ra_{CH}^{-2} + 2.873 Ra_{CH}^{-0.5})^{0.5} \quad (19)$$

Our numerical results and the values predicted by their correlation are shown in Fig. 11. It can be found that the results are generally much lower than that predicted by their correlation. The reasons accounting for this difference are as follows: (1) the fluid flowing into the channel cannot be cooled as perfectly as that in an infinite space; (2) the drag force of the natural convection in infinite space is much greater than that in an enclosure, so the fluid flow in an enclosure channel is much weaker; (3) when the double-vortex structure occurs, the

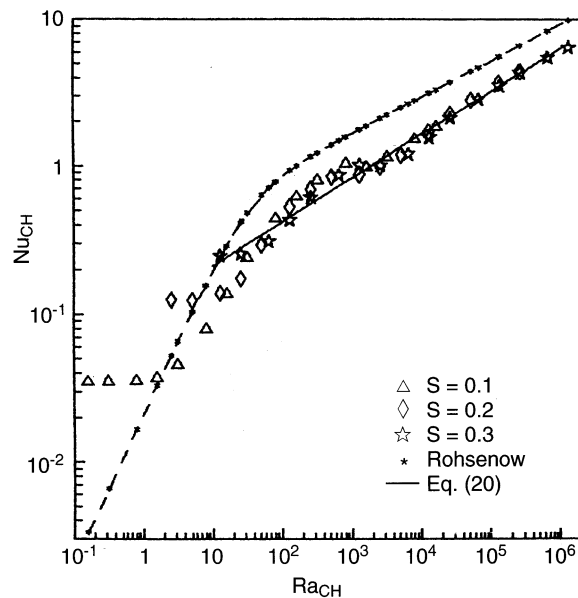


Fig. 11. Comparison of channel Nusselt number vs. channel Rayleigh number

existence of the top vortex restricts the fluid flowing through the channel. At large  $Ra_{CH}$ , the numerically predicted Nusselt number for an enclosure channel may be only as large as 60% of that for the channel situated in infinite space.

Our numerical results can be well-fitted by the following correlation when  $Ra_{CH} > 103$ :

$$Nu_{CH} = 0.2141 Ra_{CH}^{0.2961} \quad (0.1 \leq S \leq 0.3, \quad 103 \leq Ra_{CH} \leq 106) \quad (20)$$

The largest deviation between the numerical data and Eq. (20) is about 10% (see Fig. 11).

Besides, if we define the outside channel Nusselt number as

$$Nu_{CH}^* = 2Nu_0 \left( \frac{2s}{h} \right) = 4Nu_0 S \quad (21)$$

then the heat transfer characteristics on the outside wall of the plate can be well fitted as the following correlation when  $Ra_{CH} > 103$ :

$$Nu_{CH}^* = 0.3116 Ra_{CH}^{0.2698} \quad (0.1 \leq s \leq 0.3, \quad 103 \leq Ra_{CH} \leq 106) \quad (22)$$

The largest deviation is about 10% (see Fig. 12)

#### 4

#### Conclusions

In this paper, the steady-state natural convection in a rectangular cavity with an internal isolated vertical channel has been numerically investigated in the Rayleigh number range from  $1 \times 10^2$  to  $1 \times 10^7$ ,  $Pr=0.7$  and the relative channel width from 0.1 to 0.3. The following conclusions may be obtained.

1. The average Nusselt number of a vertical channel situated in an enclosure is generally lower than that of a vertical plate or a vertical channel in an infinite space. With the increase in the channel height-based Rayleigh number, the difference decreases.

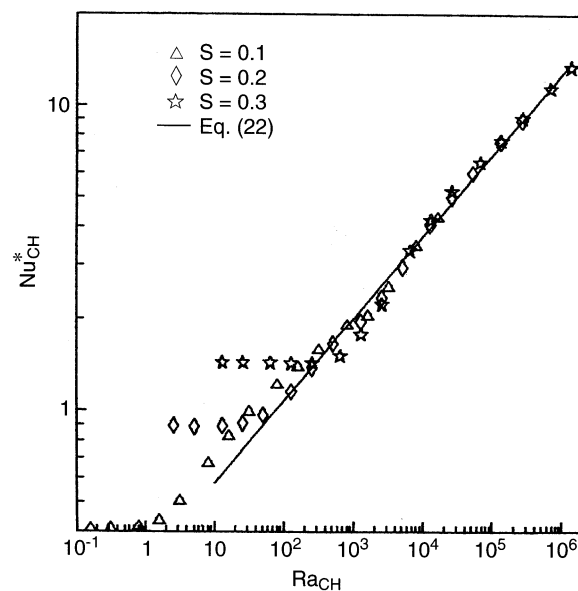


Fig. 12. Comparison of outside channel Nusselt number vs. channel Rayleigh number

2. The channel width has a significant effect on the channel inside or outside average Nusselt number in the low Rayleigh number region (for inside,  $Ra \leq 3 \times 10^4$ , for outside,  $Ra \leq 2 \times 10^2$ ). However, the increasing in the Rayleigh number leads to some insensitivity of the average Nusselt number with  $S$ .

3. For the channel Rayleigh number number greater than 103, the average channel Nusselt number of the outside wall and the inside wall for the three values of channel width may be well-correlated by Eqs. (20) and (22).

4. For the three configurations studied, the static bifurcation does exist in the Rayleigh number range from  $10^4 \sim 10^6$ , depending on the channel width  $S$ . This bifurcation is related to the transition of the single-vortex flow pattern to double-vortex one or vice versa.

#### References

1. Elenbaas, W.: Heat Dissipation of Parallel Plates by Free Convection. Vol. IX, No. 15, pp. 1–28. Physica, Amsterdam: Physica 1942
2. Bar-Cohen, A.; Rohsenow, E.M.: Thermally optimum spacing of vertical, natural convection cooled parallel plates. ASME J. Heat Transfer 106 (1984) 116–123
3. Guo, Zeng-Yuan, Wu, Xiao-Bo: Thermal drag and critical heat flux of natural convection of air in vertical parallel plates. ASME J. Heat Transfer 115 (1993) 124–129
4. Hiroshi, Nakamura; Yutaka, Asako; Takashi, Naitou: Heat transfer by free convection between two parallel plates. Num. Heat Transfer 5 (1982) 95–106
5. Sparrow, E.M.; Azevedo, L.F.A.: Vertical channel natural convection spanning between the fully-developed limit and the single-plate boundary-layer limit. Int. J. Heat Mass Transfer 28 (1985) 1847–1857
6. Chang, T.S.; Lin, T.F.: Transient buoyancy-induced flow through a heated vertical channel of finite height. Num. Heat Transfer 16, Part A (1989) 15–38
7. Naylor, D.; Floryan, J.M.; Tarasuki, J.D.: A numerical study of developing free convection between isothermal vertical plates. ASME J. Heat Transfer 113 (1991) 620–626

8. Wang, Q.W.; Yang, M.; Tao, W.Q.: Natural convection in a square enclosure with an internal isolated vertical plate. *Wärme -und Stoffübertragung* 29 (1994) 161–169
9. Adlam, J.H.: Computation of two-dimensional time-dependent natural convection in a cavity where there are internal bodies. *Comput. Fluids* 14 (1986) 142–157
10. Shyy, W.; Rao, M.M.: Simulation of transient natural convection around an enclosed vertical channel. *ASME J. Heat Transfer* 115 (1993) 946–954
11. Yang, M.; Tao, W.Q.: A numerical study of natural convection heat transfer in a cylindrical enclosure with internal concentric slotted hollow cylinder. *Num. Heat Transfer* 22, Part A (1992) 289–306
12. Churchill, S.W.; Chu, H.H.S.: *Int. J. Heat Mass Transfer* 8 (1975) 1323–1329
13. Yang, M.; Tao, W.Q.: Three dimensional natural convection in an enclosure with an internal isolated vertical plate, *ASME J. Heat Transfer* 117 (1995) 619–625